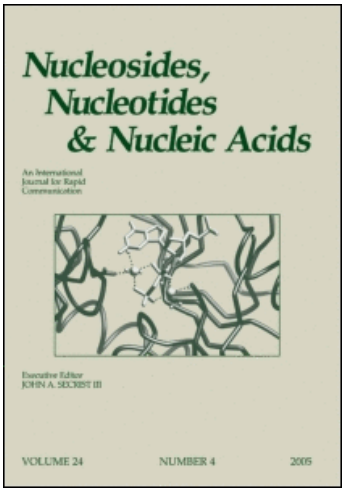

Nucleosides, Nucleotides and Nucleic Acids
Publication details, including instructions for authors and subscription information:
http://www.informaworld.com/smpp/title~content=t713597286

Structural Properties of the Neutral and Monoanionic Forms of Xanthosine, Highly Relevant to Their Substrate Properties with Various Enzyme Systems

Jarosław Poznanski[a]; Borys Kierdaszuk[b]; David Shugar[ab]
[a] Institute of Biochemistry and Biophysics, Polish Academy of Sciences, Warszawa, Poland [b] Department of Biophysics, Institute of Experimental Physics, University of Warsaw, Warszawa, Poland

Online publication date: 05 December 2003

To cite this Article Poznanski, Jarosław , Kierdaszuk, Borys and Shugar, David(2003) 'Structural Properties of the Neutral and Monoanionic Forms of Xanthosine, Highly Relevant to Their Substrate Properties with Various Enzyme Systems', Nucleosides, Nucleotides and Nucleic Acids, 22: 3, 249 — 263
To link to this Article: DOI: 10.1081/NCN-120021425
URL: http://dx.doi.org/10.1081/NCN-120021425

NUCLEOSIDES, NUCLEOTIDES & NUCLEIC ACIDS
Vol. 22, No. 3, pp. 249–263, 2003

Structural Properties of the Neutral and Monoanionic Forms of Xanthosine, Highly Relevant to Their Substrate Properties with Various Enzyme Systems

Jarosław Poznanski,[1,*] Borys Kierdaszuk,[2] and David Shugar[1,2]

[1]Institute of Biochemistry and Biophysics, Polish Academy of Sciences, Warszawa, Poland
[2]Department of Biophysics, Institute of Experimental Physics, University of Warsaw, Warszawa, Poland

ABSTRACT

The monoanions of the 6-oxopurines guanine (Gua) and hypoxanthine (Hx), and their nucleosides, $pK_a \approx 9$ due to dissociation of the N(1)-H, are predominantly in their neutral forms at physiological pH. By contrast, the monoanions of the 6-oxopurine xanthine (Xan) and xanthosine (Xao), were long ago proposed to involve dissociation of the N(3)-H, with pK_a values of 7.5 and 5.7, respectively, so that, at physiological pH, the former is mixture of the neutral and monoanionic species, and the latter predominantly the monoanion. We have employed multi-dimensional heteronuclear NMR spectroscopy, which fully confirms the proposed mode of monoanion formation in Xao (and, by implication, in Xan), further supported by the results of ab initio quantum mechanical calculations, and additionally extended to determination of the preferred conformational parameters in solution for the neutral and monoanionic species. These findings are highly relevant to the modes of binding, and to the substrate properties, of Xan, Xao and its 5′-phosphate (XMP) in numerous enzyme systems, hitherto virtually ignored, and illustrated by several concrete examples.

*Correspondence: Jarosław Poznanski, Institute of Biochemistry and Biophysics, Polish Academy of Sciences, 5a Pawinskicgo St., 02-106 Warszawa, Poland; Fax: +(48)-39121623; E-mail: jarek@ibb.waw.pl.

DOI: 10.1081/NCN-120021425
1525-7770 (Print); 1532-2335 (Online)

MARCEL DEKKER, INC.
270 Madison Avenue, New York, New York 10016

Key Words: Xanthosine; Xanthine; Monoanions; Structures; Conformation; Biological properties.

INTRODUCTION

Xanthine (Xan), Xanthosine (Xao) and its nucleotides, and some of their N-methyl congeners, are substrates and/or intermediates for numerous enzymes and enzyme systems, some of which are referred to below. It is, consequently, of interest that the unusual structural properties of these compounds in aqueous medium, particularly of the monoanionic form of the heterocyclic base, have been virtually overlooked or ignored. By analogy with the 6-oxopurines guanine (Gua) and hypoxanthine (Hx), which exist predominantly in the neutral forms at physiological pH (pK_a values about 9, see Sch. 1), early studies proposed that formation of the monoanion of xanthine also involves dissociation of the N(1)-H, currently still regarded as valid.[1,2] It was first proposed by Cavallieri et al.[3] from spectrophotometric titrations with appropriate N-methyl analogues, that the monoanion of xanthine, and the xanthine base in xanthosine, is due to dissociation of the N(3)-H, subsequently supported by Roy & Miles[4] with the aid of infrared spectroscopy. Furthermore, xanthine, with a $pK_a \approx 7.5$, is a 1:1 mixture of the neutral and monoanionic species at physiological pH; whereas xanthosine, and also XMP,[4] with a reported $pK_a \approx 5.7$, must exist predominantly as the monoanions under these conditions

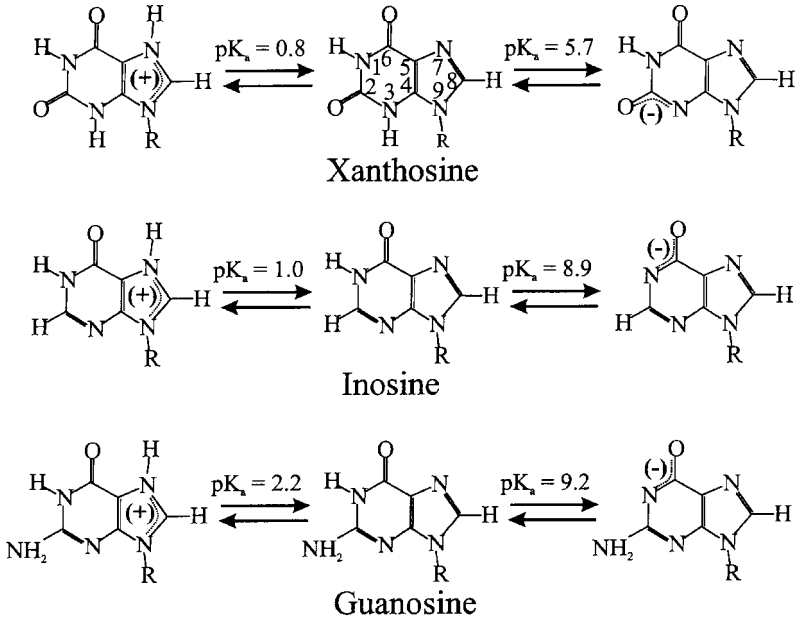

Scheme 1. Solution structures of the cationic (left), neutral (center) and monoanionic (right) forms of xanthosine, inosine and guanosine.

(see Sch. 1). The relevance of this to the enzymatic substrate properties of these compounds appears obvious, but, with one possible exception in the case of xanthine and 1-methylxanthine (see below), has been universally overlooked.

We herein present the results of a study of the solution properties of the neutral and monoanionic species of xanthosine in aqueous medium, with the aid of multidimensional NMR spectroscopy, as well as by ab initio quantum mechanical calculation, which confirm the findings of Cavalieri et al.[3] and Roy & Miles,[4] and extend this to include also data on the preferred conformations of the neutral and ionic forms. The relevance of these findings to some enzymatic reactions involving xanthine and its glycosides, recently illustrated in the case of purine nucleoside phosphorylases (PNP),[5] is briefly discussed. Our data should additionally prove helpful in investigations on the interactions of the neutral and monoanionic forms of Xan, Xao and XMP with various enzymes in solution by means of NMR spectroscopy.

EXPERIMENTAL

Materials

Xanthosine was a product of Serva (Heidelberg), homogeneous on TLC with several solvent systems, and with pH-dependent UV spectra in accord with those reported by Cavalieri et al.[3] It should be noted that the same product from three other commercial sources was found by TLC and pH-dependent UV spectra to exhibit UV-absorbing contaminants. DMSO-$^2H_6$($>99.8\%$ ^2H), NaO^2H ($>95\%$ ^2H), ^2HCl ($>95\%$ ^2H) and D_2O ($>99.8\%$ ^2H) were from Glaser AG (Basel).

Methods

All NMR experiments were carried out on a Varian Unity plus 500 MHz spectrometer at 298 K for ~8 mM Xao in DMSO, or ~1 mM Xao in D_2O.

The 2D ^1H-^{13}C HSQC spectra in DMSO were acquired with broadband decoupling. The delays $1/(2^1J_{CH})$ were tuned to obtain optimum excitation for 90 Hz (one bond) as well as 6 and 3 Hz (long range) heteronuclear coupling. The carrier was positioned at 4.8 ppm for protons and 95 ppm for carbons. The spectral width was 6000 Hz in the proton, and 18000 Hz in the carbon, dimension, respectively, and 512 t1 increments of 512 complex data points were collected. For each FID, 64 scans were averaged with a repetition delay of 1.2 s.

The 2D ^1H-^{15}N HSQC spectra in DMSO were similarly acquired. The delays $1/(2^1J_{NH})$ were tuned to obtain optimum excitation for 95 Hz (one bond) as well as 6 and 2.5 Hz (long range) heteronuclear coupling. The carrier was positioned at 116 ppm for nitrogens with the spectral width 1500 Hz.

2D ROESY experiments in DMSO and D_2O solutions were carried out in the hypercomplex mode with a spectral width of 6000 Hz, using a 300 ms mixing time with 1.2 s relaxation delay. The carrier frequency was set at 4.8 ppm, and 512 increments of 2048 complex points with 480 transients were used.

MARCEL DEKKER, INC.
270 Madison Avenue, New York, New York 10016

2D COSY experiments in DMSO and D_2O solutions were carried out in the hypercomplex mode with a spectral width of 6000 Hz and 1 s relaxation delay. The carrier frequency was set at 4.8 ppm and 450 increments of 1024 complex points with 64 transients were used.

1D spectra were processed and analyzed with the help of the MestRe-C 2.3 program.[6] ^{13}C spectra were transformed using a Gaussian filter, resulting in 3 Hz resonance broadening. For ^{1}H spectra either $\pi/4$ shifted or pure sine-bell (for precise coupling constant determination) filters were used.

2D spectra were processed by NMRPipe,[7] using a $\pi/4$ shifted sine-bell filter and zero filling up to 1024 data points in the t1 dimension prior to Fourier transformation. The spectra were analyzed with the X-Easy program.[8]

Resonance assignments for Xao in DMSO were based on a combination of ^{1}H-^{13}C and ^{1}H-^{15}N heteronuclear HSQC[9] spectra coupled with 2D-COSY[10] and 300 ms mixing time 2D-ROESY[11] experiments. Titration of Xao in D_2O solution was conducted by both ^{13}C and ^{1}H 1D spectroscopy, following proton resonance assignments by a combination of 2D-ROESY and 2D-COSY spectra. ^{13}C assignments in D_2O solution were adapted from those in DMSO.

Titrations were conducted on $\sim$1 mM solutions of Xao in aqueous medium, adjusted to appropriate pH values at intervals of 0.1–0.3 units with the aid of 100 mM NaO^2H and ^2HCl. Chemical shifts of the resonances were plotted according to a modified Henderson-Hasselbach equation:

$$\Delta\delta_i = \Delta_i \frac{10^{n(pK_a - pH)}}{1 + 10^{n(pK_a - pH)}}$$

where $\Delta\delta_i$ is the chemical shift change of the i-th resonance at a given pH, Δ_i is the change in chemical shift of the i-th proton on dissociation, n is a Hill coefficient, and pK_a is the apparent ionization constant. The values of n and pK_a were kept identical for all titration curves.

Precise coupling constants were obtained using ISSSS,[12] based on the improved LAOCOON II algorithm.[13] Conformational analysis of the ribose ring puckering was made with the help of software based on the Altona algorithm for sugar ring pseudorotation.[14]

Spectrophotometric Titration of Xao in Strongly Acidic Medium

This was performed with a Varian 50-Bio spectrophotometer, equipped with a thermostated (25°C) cell holder. HCl was used for adjustment of pH in the range -1 to 2, and acetate buffers in the range 3.5–4.7.

Measurements of pH

These were carried out with an accuracy of ± 0.05 using CP315m pH meter (Elmetron, Poland) equipped with a combination semimicro electrode (Orion, UK) and temperature sensor.

Marcel Dekker, Inc.
270 Madison Avenue, New York, New York 10016

Calculated Free Energy Difference Between Monoanionic Forms

The difference between species with dissociation of the N(1)-H or N(3)-H was estimated at the quantum mechanical level for the model 9-methyxanthine, the structure of which was initially optimized by energy minimization in vacuo with the Sybyl package, using the Tripos forcefield[15] with Amber atomic charges.[16] This was followed by ab initio analysis with the aid of the GAMESS 6.0 program,[17] using restricted Hartree-Fock formalization (RHF) with the 6-31G(d,p) basis set[18] and the B3LYP functional.[19] Initially the structures of both Xao monoanions were optimized by in vacuo calculations. Then wave functions and coordinates were reoptimized using the PCM approach,[20] permitting computation of solute-solvent electrostatic interactions in the presence of polarizable continuum. In the PCM method the solute was placed in a cavity formed by a set of spheres centered on each atom with a radius 1.2 times larger than the Van der Waals radius. Renormalization of the wave functions was performed to compensate for penetration of the solute charge density outside the cavity. Dispersion end repulsion corrections[22] were also included in the self-consistent wave function. Finally, according to the Clavarie-Pierotti model,[21] cavitation corrections were applied. No corrections for zero state vibration were done. Calculations were performed independently for aqueous and DMSO solutions, using the following sets of parameters: dielectric constant (ε) 78.39; solvent radius (R_{solv}) 1.385 Å; solvent partial molar volume (V_{mol}) 18.07 cm^3/mol; the thermal expansion coefficient (TCE) 0.257E–03 K^{-1}; surface tension (σ) 71.81 dyn/cm; the thermal coefficient of surface tension logarithm ($\Delta\sigma$) 0.65; the cavity microscopic coefficient (CMF) 1.277 for aqueous medium; and $\varepsilon = 46.70$; $R_{solv} = 2.455$ Å; $V_{mol} = 70.94\ cm^3$/mol; TCE = 0.982E–01 K^{-1}; $\sigma = 42.86$ dyn/cm; $\Delta\sigma = 0.00$; CMF = 0.000 for DMSO.

RESULTS AND DISCUSSION

Proton Assignments in DMSO Solution

This was based on 2D-COSY experiments, and led to unequivocal assignments of H(8) and all ribose protons. One of the ring nitrogen protons, located at 11.73 ppm, is strongly broadened (halfwidth ~200 Hz), whereas the other, located at 10.87 ppm, is relatively narrow (3.9 Hz). Absence of magnetization transfer from the narrow resonance to the ribose protons by 2D-ROESY (Fig. 1) led to identification of the narrow resonance signal as the N(1)-H, located distally from all the sugar protons, while relaxation of the slowly exchanging N(3)-H proton at 11.73 ppm precludes efficient magnetization transfer to the neighbouring ribose H(1′), H(2′) and H(3′). Addition of a small amount of water (≈10 μL) to the DMSO solution did not affect the N(1)-H resonance, whereas the N(3)-H signal disappeared due to rapid proton exchange (not shown). It follows that, in aqueous medium as well, the N(3)-H proton is the more labile.

MARCEL DEKKER, INC.
270 Madison Avenue, New York, New York 10016

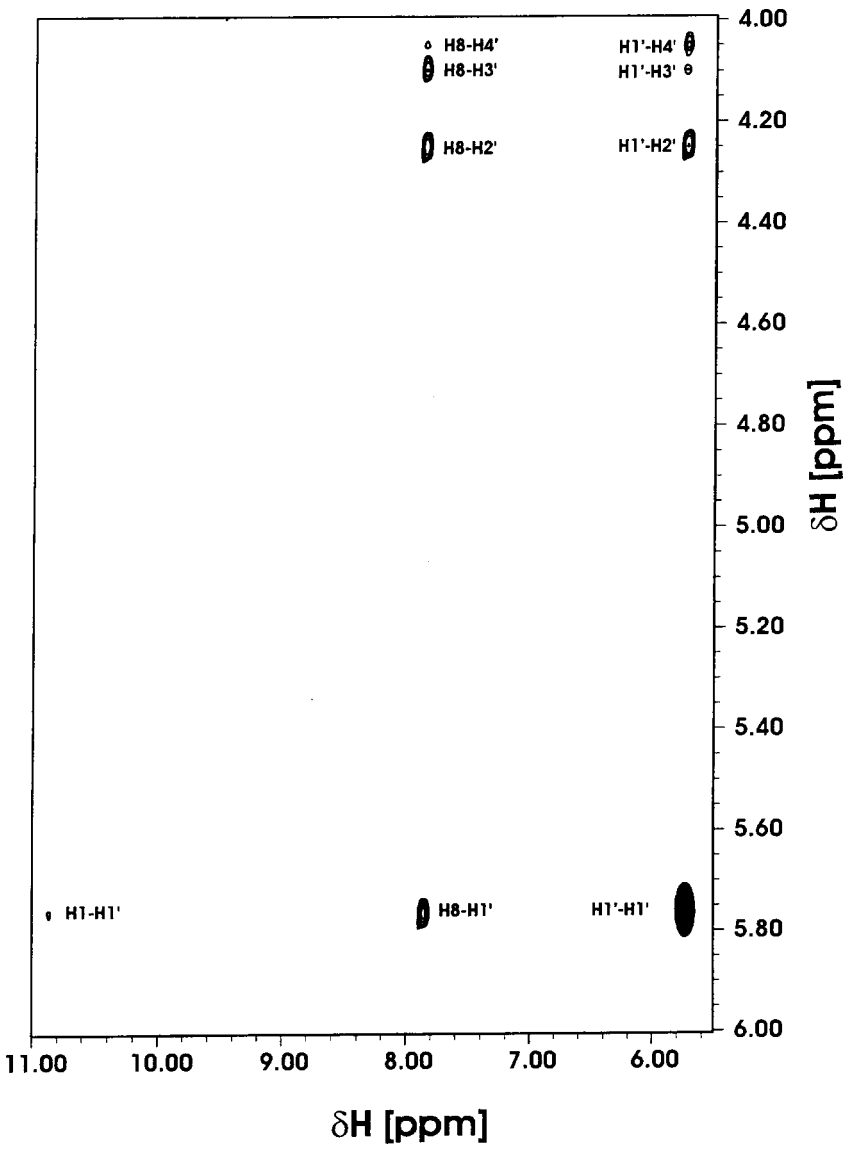

Figure 1. Part of 2D-ROESY spectrum of Xao recorded in DMSO solution. Absence of non-diagonal crosspeaks for the 10.87 ppm signal, when a number of C(8)-H crosspeaks are clearly observed, indicates that its assignment is the N(1)-H distal from the sugar moiety. The N(1)-H -H1′ crosspeak volume is two orders of magnitude lower than that of C(8)-H-H1′. The H1′ diagonal peak is denoted by the black ellipse.

Marcel Dekker, Inc.
270 Madison Avenue, New York, New York 10016

Carbon and Nitrogen Resonances

These were assigned on the basis of a series of ^{15}N-^{1}H and ^{13}C-^{1}H HSQC spectra. The observed cross-peaks pattern (Fig. 2) is consistent with the final assignments listed in Table 1.

Titration of Xanthosine by ^{1}H Spectroscopy

Titration was conducted over the pH range 1.5–9.0, and demonstrated detectable pH-dependent changes in chemical shifts of all proton signals except H3′ (Fig. 3). With the use of Eq. (1), the pK_a for dissociation of the N(3)-H was estimated as 5.48 ± 0.18, as compared to a reported value of 5.50 ± 0.05 obtained by spectrophotometric titration.[3] This is also consistent with a value of 5.85 for 1-methylxanthosine, and 6.15 for O^6-methylxanthosine [4] both of which possess only one ionizable proton, at N(3).

Titration to lower pH values (Fig. 3) revealed an additional ionic equilibrium with a $pK_a < 1$, clearly due to protonation. A more accurate value was obtained by spectrophotometric titration, leading to a $pK_a = 0.0 \pm 0.1$. Bearing in mind the marked chemical shift of H(1′), and the very large chemical shift of H(8), accompanying titration (Fig. 3, left-hand side), it is clear that protonation occurs on the N(7) nitrogen.

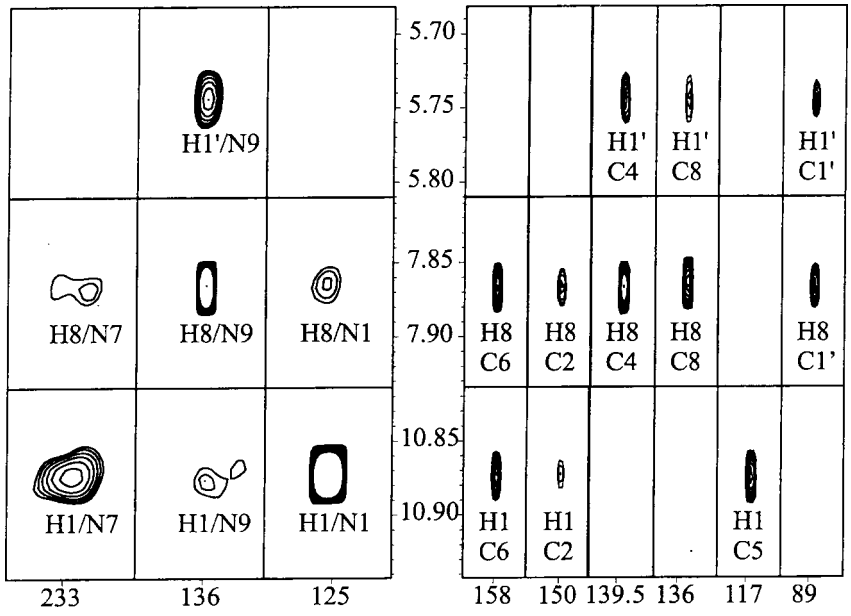

Figure 2. Heteronuclear correlation patterns derived from ^{15}N-^{1}H HSQC (left) and ^{13}C-^{1}H HSQC (right) spectra of xanthosine in DMSO solution.

Table 1. Carbon, nitrogen and proton signal assignments for xanthosine in DMSO, and for its neutral, monoanionic, and cationic forms in aqueous medium.

	DMSO		Water				
			(pH 1)	Neutral (pH 4)		Anion (pH 8.6)	
	Heavy atom	Proton	Proton	Heavy atom	Proton	Heavy atom	Proton
N1	125.2 (145.5[a])	10.87 (10.7[b])					
C2	150.4 (151.5[c])						
N3		11.73 (11.9[b])					
C4	139.3 (140.4[c])						
C5	116.3 (117.4[c])					116.2	
C6	157.9 (158.9[c])					153.4	
N7	233.5 (233.4[a])						
C8	135.7 (136,7[c])	7.87 (7.85[c])			7.85	138.1	7.79
N9	136.2 (167.4[a])						
C1′	88.7 (89.9[c])	5.74 (5.77[c])	5.90	92.6	5.82	88.9	5.78
C2′	73.9 (75.1[c])	4.22 (4.24[c])	4.52	76.6	4.45	73.9	4.75[d]
C3′	70.8 (71.9[c])	4.07 (4.10[c])	4.38	73.6	4.32	71.8	4.31
C4′	86.1 (87.2[c])	4.02 (4.04[c])	4.32	89.0	4.25	86.8	4.17
C5′	61.2 (62.3[c])	3.66 (3.69[c])	3.92	63.7	3.86	62.4	3.81, 3.71

[a]Average chemical shifts of guanosine ^{15}N nitrogen resonances estimated from data in the BMRB data bank (http://www.bmrb.wisc.edu/).
[b]These values are for 9-methylxanthine[40].
[c]Data obtained from SDBSWeb (http://www.aist.go.jp/RIODB/SDBS)[41].
[d]Signal under water resonance.

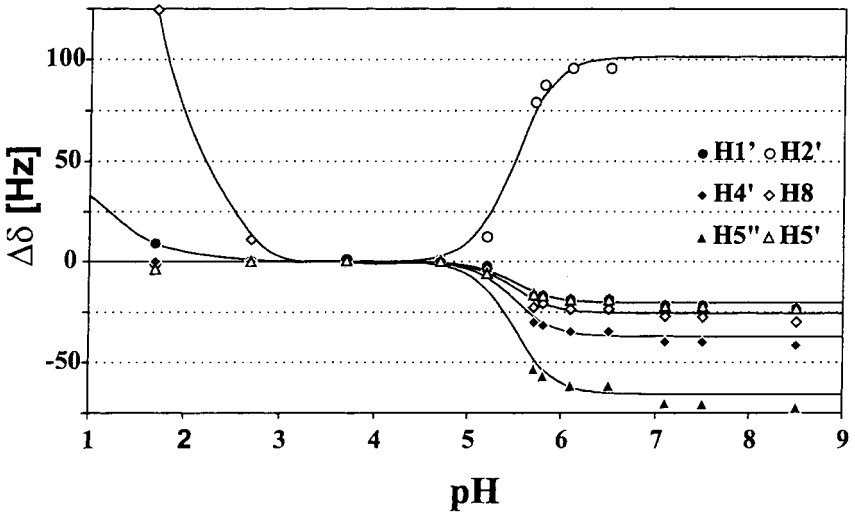

Figure 3. pH-dependence of proton chemical shift drifts in xanthosine. Note that H3′ is invariant with pH (not shown).

Marcel Dekker, Inc.
270 Madison Avenue, New York, New York 10016

pH-Dependence of Conformational Equilibrium

From Fig. 3, it will be noted that the largest changes in chemical shifts, in going from the neutral form of Xao to the monoanionic species, is observed for H2′. This is reminiscent of an earlier report, based on the use of model purine nucleosides, that large changes in chemical shifts of H2′ are associated with a change in the *syn-anti* equilibrium.[23]

Comparison of the 2D-ROESY spectra of Xao at pH 4 (neutral form) and pH 8 (monoanion) demonstrate a significant change of the cross-peak pattern characteristic for the *syn-anti* equilibrium. Thus, at pH 4, the NOE effects for H8-H1′, H8-H2′ and H8-H3′ magnetization transfers are in ratio 5:1:1; whereas, at pH 9, H8-H1′ and H8-H3′ magnetization transfers are in the ratio 3:1 (the H2′ resonance is located under water, and the NOE effect is strongly distorted). The overall data clearly indicate that the population of the anti conformer is significantly increased upon dissociation of the N(3) proton.

Analysis of the pH-dependence of the furanose ring puckering shows that dissociation of the N(3) proton results in lower destabilization of the N type conformer (Fig. 4, ~5% at pH 4 vs. 15% at pH 9), accompanied by a small increase of the mean pseudorotation amplitude τ (29° at pH 4 vs. 32.3° at pH 9).

Analogously, the rotational equilibrium of the exocyclic C(5′) group is coupled with the ionic form of the base. Despite the fact that the H5′ and H5″ signals overlap, precluding detailed analysis, it may be concluded that dissociation of the N(3) proton significantly affects the conformational equilibrium of the C(5′)H_2OH group, reflected by an increasing population of the *gauche* rotamer (Fig. 4).

Summing up, we propose the following model for the pH-dependence of the conformation. The extremely low magnetization transfer from the narrow base imino proton signal to the sugar protons (Fig. 1) indicates that the N(3)-H undergoes significant exchange on the NMR time-scale resulting in large broadening of the signal in DMSO solution. Dissociation of the N(3)-H proton stabilizes the *anti* conformation. Variation of the *syn-anti* equilibrium modifies interaction between the base and sugar, leading to an increase in population of the N puckering form, and an increase in the mean pseudorotation amplitude due to decreased steric interactions between the sugar ring and the base. Furthermore, a change in the *syn-anti* equilibrium results in a change in rotational equilibrium of the exocyclic group. These tendencies are in accord with crystallographic data, which show the *syn* conformer of the neutral form stabilized by an intramolecular N(3)-H—O-C(5′) hydrogen bond.[24] The estimated solution conformation of neutral Xao ($\tau = 32.3$, $S = 95\%$) agrees with the crystal conformation ($\tau = 38.7$, $P = 156°$, respectively).

Quantum Mechanical Calculations

Preliminary ab initio analysis demonstrated stabilization of the N(3) dissociated form relative to N(1) by 26 kcal/mol in vacuo. Consequently, in both DMSO and aqueous medium, the internal free energy significantly favors N(3)-H dissociation, notwithstanding that solute-solvent electrostatic interactions favour the N(1) dissociated form. Other contributions to the free energy are almost identical for both

MARCEL DEKKER, INC.
270 Madison Avenue, New York, New York 10016

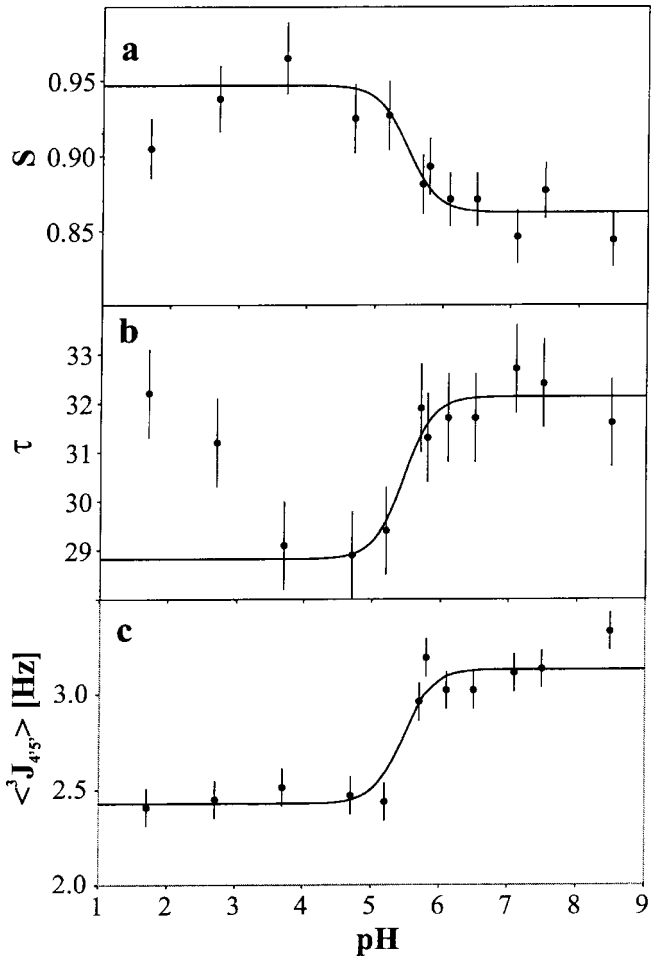

Figure 4. pH-dependence of the pentose ring pucker of xanthosine: (a) fraction of S form; (b) mean pseudorotation amplitude τ; (c) mean C(4′)-H, C(5′)-H vicinal coupling constant.

forms. Finally, the N(3)-dissociated form is stabilized by 10 kcal/mol and 11 kcal/mol in DMSO and aqueous solution, respectively. The calculated results (see Table 2) are in accord with the NMR assignments made for Xao in DMSO solution, which demonstrated that the N(3), and not the N(1), proton is by far the more labile. In line with this, earlier theoretical studies demonstrated that the monoanion of 6-thioxanthine involves dissociation of the N(3)-H, as also for the parent xanthine.[25]

BIOLOGICAL ASPECTS

Xan, Xao and XMP, as well as some of their N-methyl analogues, are substrates or intermediates for a large number of enzymes or enzyme systems.[5] For example,

Marcel Dekker, Inc.
270 Madison Avenue, New York, New York 10016

Table 2. Free energy partition estimated for the two monoanionic forms of Xanthosine in DMSO and in aqueous medium, from ab initio calculations with the Polarizable Continuum Model extended for cavitation, repulsion, and dispersion interactions.

Energy partition (kcal/mol)	DMSO			Water		
	H1 diss	H3 diss	Δ	H1 diss	H3 diss	Δ
Internal energy in vacuo and ΔE^o	−375055.79	−375082.20	**26.41**	−375055.79	−375082.20	**26.41**
Internal energy in solvent	−375043.37	−375064.02	20.65	−375042.89	−375075.46	32.57
Free energy in solvent	−375149.28	−375159.43	10.15	−375150.43	−375161.27	10.84
Electrostatic interaction	−92.41	−82.14	−10.27	−94.02	−72.50	−21.52
Pierotti cavitation energy	21.07	20.94	0.13	21.68	21.52	0.16
Dispersion free Energy	−17.70	−17.46	−0.24	−17.75	−17.56	−0.19
Repulsion free energy	4.20	4.19	0.01	4.23	4.25	−0.02
Total solute-solvent interaction	−84.84	−74.48	−10.36	−85.86	−64.29	−21.57
Total free energy in solvent and ΔG^o	−375128.21	−375138.49	**10.28**	−375128.75	−375139.75	**11.00**

IMP dehydrogenase, the rate-limiting enzyme in de novo synthesis of guanine nucleotides, catalyzes the NAD-dependent oxidation of IMP to XMP, which is then converted to GMP.[26] Xan and Xao are weak to moderate substrates of mammalian purine nucleoside phosphorylases (PNP), dependent, as expected, on the pH,[5] but not of the corresponding enzyme from *E. coli* encoded by the *deoD* gene (referred to as PNP-I). But cultivation of *E. coli* cells in the presence of Xao leads to induction of a new enzyme, PNP-II, encoded by the *XapA* gene, with a high preference for both Xan and Xao.[27]

The biosynthesis of caffeine, recently extensively reviewed,[28] proceeds through a number of enzymatic steps involving as intermediates Xan, Xao, XMP, and N(7)-methyl-XMP, followed by cleavage of the latter and stepwise enzymatic methylation of the liberated N(7)-methyl-Xan to give trimethylxanthine (caffeine). A nucleoside triphosphate pyrophosphorylase from a thermophile, *Methanococcus jannaschii*, is highly specific for ITP and XTP, particularly at alkaline pH,[29] where both exist exclusively as the monoanions, albeit with different structures, not noted by the authors. Xanthine derivatives are under active investigation as activators of the CFTR chloride channel, defects in which are known to underlie cystic fibrosis.[30]

Particularly relevant are purine phosphoribosyltransferases, which includes a family of enzymes specific for 6-oxopurines. The human enzyme accepts Hx and Gua, but only minimally Xan,[31,32] whereas *E. coli* contains two such enzymes, one with a preference for Hx and Gua, the other for Gua and Xan.[33] Some parasitic protozoa, e.g. *Leishmania donovani*, possesses one such enzyme, with a marked preference for Xan.[34,35]

It is surprising, in fact quite extraordinary, that in all the foregoing, and in many other enzyme systems, no reference is made to either the unusual structure of the monoanion of free Xan, or of the xanthine moiety of Xao and XMP, or the fact that, at physiological pH, Xan is a mixture of the neutral and monoanionic forms, and Xao and XMP exist almost exclusively with their Xan moiety as the monoanion.

We are aware of only one enzyme system, xanthine oxidase, where attention was directed to possible substrate properties of the monoanion of Xan. From kinetic and pH-dependence studies, it was proposed that the neutral forms of Xan[1] and N(1)-methyl-Xan[2] are the preferred substrates, but with the erroneous assumption that monoanion formation is due to dissociation of an imidazole proton. And, in our opinion, weak substrate properties of the monoanions were not unequivocally excluded.

Reverting to the purine phosphoribosyltransferases, referred to above, crystal structures of many of these, in complexes with 6-oxopurines or their nucleotides, including Xan and XMP, have been reported. The modes of binding of Hx and Gua in the forward reaction, and of IMP and GMP in the reverse reaction, have been reasonably well assigned. But the situation is much less clear for binding of Xan and XMP,[33] in part, perhaps, because resolution of crystal structures is insufficient to distinguish between a C=O bond and a C-O^-. It is, of course, conceivable that binding of Xan or XMP to the enzyme in the crystalline state may result in liquidation of dissociation; but it was long ago reported that the crystal structure of the monoanion of Xan shows the N(3)-H to be dissociated.[36] At the polymer level, it has been shown that poly(xanthylate) forms multi-stranded helices with different structures in acid and alkaline media, related to dissociation of the N(3)-H of the Xan residues,[37,38] and confirmed by X-ray diffraction of poly(X) fibres, which form one helix at acid pH with the Xan residues in the neutral 2,4-diketo form, and a different one at pH 8, in which the N(3)-H of the Xan residues is dissociated.[39] The fact remains that crystallographers appear to be unaware of the structure and ionic properties of Xan and XMP in solution at the physiological pH at which these enzymes are optimally active.

ACKNOWLEDGMENTS

We are indebted to Dr. Michał Wojciechowski for consultations on the theoretical calculations and to the Laboratory of Biological NMR of IBB-PAN for access to the NMR spectrometer. This study was supported by the Polish State Committee for Scientific Research (KBN), including individual grants and BST-718/BF.

ABBREVIATIONS

Xan	xanthine
Xao	xanthosine
XMP	xanthosine-5′-phosphate
PNP	purine nucleoside phosphorylase

REFERENCES

1. Kim, J.H.; Ryan, M.G.; Knaut, H.; Hille, R. The reductive half-reaction of xanthine oxidase. The involvement of prototropic equilibria in the course of the catalytic sequence. J. Biol. Chem. **1996**, *271*, 6771–6780.
2. Sau, A.K.; Mondal, M.S.; Mitra, S. Effects of pH and temperature on the reaction of milk Xanthine oxidase with 1-methylxanthine. J. Chem. Soc. Dalton Trans. **2000**, *20*, 3688–3692.
3. Cavalieri, L.; Fox, J.; Stone, A.; Chang, N. On the nature of xanthine and substituted xanthines in solution. J. Am. Chem. Soc. **1954**, *76*, 1119–1122.
4. Roy, K.B.; Miles, H.T. Tautomerism and ionization of xanthosine. Nucleosides and Nucleotides **1983**, *2*, 231–242.
5. Stoychev, G.; Kierdaszuk, B.; Shugar, D. Xanthosine and xanthine: Substrate properties with purine nucleoside phosphorylases, and relevance to other enzyme systems. Eur. J. Biochem. **2002**, *269*, 4048–4057.
6. Cobas, C.; Cruces, J.; Sardina, F.J. MestRe-C 2.3a, Magnetic Resonance Companion NMR Data Processing Program. Departamento de Química Orgánica, Facultad de Química, Universidad de Santiago de Compostela, 1706 Santiago de Compostela Spain.
7. Delaglio, F.; Grzesiek, S.; Vuister, G.W.; Zhu, G.; Pfeifer, J.; Bax, A. NMRPipe: A multidimensional spectral processing system based on UNIX pipes. J. Biomol. NMR. **1995**, *6*, 277–293.
8. Bartels, C.; Xia, T.-E.; Billeter, M.; Guntert, P.; Wüthrich, K. The Program XEASY for the computer-supported NMR spectral analysis of biological macromolecules. J. Biol. NMR **1995**, *5*, 1–10.
9. Bodenhausen, G.; Roben, D.J. Natural abundance Nitrogen-15 NMR by enchanced heteronuclear spectroscopy. Chem. Phys. Lett. **1980**, *69*, 185–189.
10. Hurd, R.E. Gradient-enhanced spectroscopy. J. Magn. Reson. **1990**, *87*, 422–428.
11. Bothner-By, A.; Lee Stephens, J.; Warren, C.; Jeanloz, R. Structure determination of a tetrasaccharide: Transient nuclear overhauser effects in the rotating frame. J. Am. Chem. Soc. **1984**, *106*, 811–813.
12. Poznański, J. *Iterative Seven Spin System Simulation*, Program made within the Biosym research fellowship on a field of NMR software.
13. Gunther, H. *NMR Spectroscopy*; John Wiley and Sons: Chichester, 1980.
14. de Leeuw, H.P.M.; Haasnoot, C.A.G.; Altona, C. Empirical correlations between conformational parameters in β-D-furanoside fragments derived from a statistical survey of crystal structures of nucleic acid constituents. Israel J. Chem. **1980**, *20*, 108–126.

15. Clark, M.; Cramer, R.D., III; Van Opdenbosh, N. Validation of the general purpose tripos 5.2 Force Field. J. Comput. Chem. **1989**, *10*, 982–1012.
16. Weiner, J.S.; Kollman, P.A.; Case, D.A.; Singh, U.C.; Ghio, C.; Alagona, G.; Profeta, S.; Weiner, P. A new force field for molecular mechanical simulation of nucleic acids and proteins. J. Am. Chem. Soc. **1984**, *106*, 765–784.
17. Schmidt, M.W.; Baldridge, K.K.; Boatz, J.A.; Elbert, S.T.; Gordon, M.S.; Jensen, J.J.; Koseki, S.; Matsunaga, N.; Nguyen, K.A.; Su, S.; Windus, T.L.; Dupuis, M.; Montgomery, J.A. General atomic and molecular electronic structure system. J. Comput. Chem. **1993**, *14*, 1347–1363.
18. Francl, M.M.; Pietro, W.J.; Hehre, W.J.; Binkley, J.S.; Gordon, M.S.; DeFrees, D.J.; Pople, J.A. Self-consistent molecular orbital methods. XXIII. A polarization-type basis set for second-row elements. J. Chem. Phys. **1982**, *77*, 3654–3665.
19. Hertwig, R.H.; Koch, W. On the parameterization of the local correlation functional. What is Becke-3-LYP? Chem. Phys. Lett. **1997**, *268*, 345–351.
20. Cammi, R.; Tomasi, J. Remarks on the use of the apparent surface charges (ASC) methods in solvation problems: iterative versus matrix-inversion procedures and the renormalization of the apparent charges. J. Comput. Chem. **1995**, *16*, 1449–1458.
21. Langlet, J.; Claverie, P.; Caillet, J.; Pullman, A. Improvements of the continuum model. 1. Application to the calculation of the vaporization thermodynamic quantities of nonassociated liquids. J. Phys. Chem. **1988**, *92*, 1617–1631.
22. Amovilli, C.; Mennucci, B. Self-consistent-field calculation of Pauli repulsion and dispersion contributions to the solvation free energy in the polarizable continuum model. J. Phys. Chem. B **1997**, *101*, 1051–1057.
23. Stolarski, R.; Hagberg, C.E.; Shugar, D. Studies on the dynamic *syn-anti* equilibrium in purine nucleosides and nucleotides with the aid of ^{1}H and ^{13}C NMR spectroscopy. Eur. J. Biochem. **1984**, *138*, 187–192.
24. Lesyng, B.; Marck, C.; Seanger, W. The crystal structure of anhydrous xanthosine displays intramolecular O(2′)-H ... O(3′) hydrogen bond. Z. Naturforsch. **1983**, *39*, 720–724.
25. Civcir, P.U. Tautomerism of 6-thioxanthine in gas and aqueous phases using AM1 and PM3 methods. J. Chem. Phys. **2001**, *114*, 1582–1588.
26. Franchetti, P.; Grifantini, M. Nucleoside and non-nucleoside IMP dehydrogenase inhibitors as antitumor and antiviral agents. Curr. Med. Chem. **1999**, *6*, 599–614.
27. Bezirjian, Kh.O.; Kocharian, Sh.M.; Akopyan, Zh.I. Isolation of a hexameric form of purine nucleoside phosphorylase II from E. coli, Comparative study of trimeric and hexameric forms of the enzyme. Biokhimia **1986**, *51*, 1085–1092.
28. Ashihara, H.; Crozier, A. Biosynthesis and catabolism of caffeine in low-caffeine-containing species of Coffea. J. Agricult. Food Chem. **1999**, *47*, 3425–3431.
29. Chung, J.H.; Back, J.H.; Park, Y.I.; Han, Y.S. Biochemical characterization of a novel hypoxanthine/xanthine dNTP pyrophosphatase from *Methanococcus jannaschii*. Nucleic Acids Res. **2001**, *29*, 3099–3107.
30. Chappe, V.; Mettey, Y.; Vierfond, J.M.; Hanrahan, J.W.; Gola, M.; Verrier, R.; Becq, F. Structural basis for specificity and potency of xanthine

derivatives as activators of the CFTR chloride channel. British J. Pharmacol. **1998**, *123*, 683–693.
31. Vos, S.; Parry, R.J.; Burns, M.R.; de Jersey, J.; Martin, J.L. Structures of free and complexed forms of Escherichia coli xanthine-guanine phosphoribosyltransferase. J. Molec. Biol. **1998**, *282*, 875–889.
32. Shivashankar, K.; Sujay Subbayya, I.N.; Balaram, H. Development of a bacterial screen for novel Hx-Gua PRTase substrates. J. Mol. Microb. Biotechol. **2001**, *3*, 557–562.
33. Vos, S.; de Jersey, J.; Martin, J.L. Crystal structure of Escherichia coli xanthine phosphoribosyltransferase. Biochemistry **1997**, *36*, 4125–4134.
34. Craig, S.P. 3rd.; Eakin, A.E. Purine phosphoribosyltransferases. J. Biol. Chem. **2000**, *275*, 20,231–20,234.
35. Jardim, A.; Bergeson, S.E.; Shih, S.; Carter, N.; Lucas, R.W.; Merlin, G.; Myler, P.J.; Stuart, K.; Ullman, B. Xanthine phosphoribosyltransferase from Leishmania donovani. Molecular cloning, biochemical characterization, and genetic analysis. J. Biol. Chem. **1999**, *274*, 34,403–34,410.
36. Mizuno, H.; Fujiwara, T.; Tomita, K. The crystal and molecular structure of the sodium salt of xanthine. Bull. Chem. Soc. Japan **1969**, *42*, 3099–3105.
37. Fikus, M.; Shugar, D. Properties of poly-xanthylic acid and its reactions with potentially complementary homopolynucleotides. Acta Biochim. Polon. **1969**, *16*, 55–84.
38. Roy, K.B.; Frazier, J.; Miles, H.T. Polixanthylic acid: Structures of the ordered forms. Biopolymers **1979**, *18*, 3077–3087.
39. Arnott, S.; Chandrasekaran, R.; Day, A.W.; Puigjaner, L.C.; Watts, L. Double-helical structures for polyxanthylic acid. J. Mol. Biol. **1981**, *149*, 489–505.
40. Twanmoh, L.M.; Wood, H.B.Jr.; Driscoll, J.S. NMR spectral characteristics of N-H protons in purine derivatives. J. Heterocycl. Chem. **1973**, *10*, 187–190.
41. Yamamoto, O.; Someno, K.; Wasada, N.; Hiraishi, J.; Hayamizu, K.; Tanabe, K.; Tamura, T.; Yanagisawa, M. An integrated spectral data base system including IR, MS, ^{1}H-NMR, ^{13}C-NMR, ESR and Raman spectra. Anal. Sci. **1988**, *4*, 233.

Received August 28, 2002
Accepted December 26, 2002

MARCEL DEKKER, INC.
270 Madison Avenue, New York, New York 10016